

Lu, C., and Swart, P.K., 2023, The application of dual clumped isotope thermometer (Δ_{47} and Δ_{48}) to the understanding of dolomite formation: *Geology*, <https://doi.org/10.1130/G51576.1>

Supplemental Material

Methods

Figures S1–S14

Supplemental Data

Supplemental Material

The application of the dual clumped isotope thermometry analyses (Δ_{47} and Δ_{48}) to the understanding of dolomite formation

Chaojin Lu¹, Peter K. Swart¹

1. Department of Marine Geosciences, Rosenstiel School of Marine, Atmospheric and Earth Sciences, University of Miami, Miami FL 33149, USA

1. Geological Settings

The Clino core was drilled in 1989 approximately 5 km away from the edge of the Great Bahama Bank and penetrated 677 meters below the mud pit (mbmp) downcore through the platform marginal to slope and upper slope sediments (Eberli, 2000; Kenter et al., 2001; McNeill et al., 2001; Swart and Melim, 2000) (Fig. S1). The abundance of dolomite is related to the presence of marine hardgrounds such as the erosional surfaces at 367 mbmp and the depositional hiatus at 536 mbmp (Fig. S2A). The dolomite shows two main textures that include fabric-preserving texture and microsucrosic (Swart and Melim, 2000). The fabric-preserved dolomite consists of replaced micritic grains and interparticle cements. The microsucrosic dolomites are characterized by the euhedral rhombs (1 to 40 μm) replacing both matrix and cement. The formation of the Clino dolomite is considered to be contemporaneous with the duration of hardground or erosional surface and is supported by several lines of evidence (Murray et al., 2021). First, the percentage of dolomite is at a maximum immediately below the hiatus or erosional surface. Second, the Sr concentrations increase below the hiatus or erosional, a phenomenon that is visible in pore water profiles (Gieskes et al., 1986), and is a result of both calcite and dolomite formation in a semi-closed environment (Murray et al., 2021; Swart and Melim, 2000). Third, there are significant elevated the carbonate-associated sulfate (CAS) $\delta^{34}\text{S}_{\text{CAS}}$ values together with co-varied magnesium ($\delta^{26}\text{Mg}$) and calcium ($\delta^{44}\text{Ca}$) isotope values that reflect the microbial-mediated dolomitization in a closed system (Murray et al., 2021). Finally, the increasing $\delta^{18}\text{O}_{\text{fluid}}$ values below the non-depositional surfaces are consistent with the known geothermal gradient of between 35°C/km (Eberli et al., 1997).

The island of San Salvador is located near the eastern margin of the Bahamas platform (Fig. S1). The San Salvador drilling core penetrated to 168 m of Pleistocene to Miocene carbonate sediments. The chronological framework was established by biostratigraphy by Sr-isotope stratigraphy (Swart et al., 1987) and magnetostratigraphy (McNeill et al., 1988). The dolomitized interval extends from 35 to 145 m in depth and the remainder being composed of a small amount of aragonite in the upper portion of the core and low magnesium calcite (LMC) throughout the remainder (Fig. S2B). Five episodes of dolomitization, based on Sr isotopes, were suggested by Vahrenkamp et al. (1991). These include the terminal Early Miocene, Late Miocene, Late Pliocene, Pliocene to Pleistocene and Late Pleistocene. Two endmember dolomite were described, a fabric-

retentive, crystalline mimetic (CM) and fabric-destructive, microsucrosic (MS) (Dawans and Swart, 1988) which made up a series of five alternations each capped by the CM and evidence of sub-aerial exposure. The transition between CM and MS dolomites responds to the small amplitude (a few meters) of Pliocene sea-level cycles (Dawans and Swart, 1988). Based on previously published $\delta^{18}\text{O}_{\text{carb}}$, $\delta^{13}\text{C}_{\text{carb}}$, and Δ_{47} values, it was concluded that the fluid, which formed the dolomite, was the normal seawater (Murray and Swart, 2017). The relatively constant Sr concentrations and $\delta^{34}\text{S}_{\text{CAS}}$ values supported the marine dolomitization within an open system (Fig. S2B) (Dawans and Swart, 1988; Murray et al., 2021).

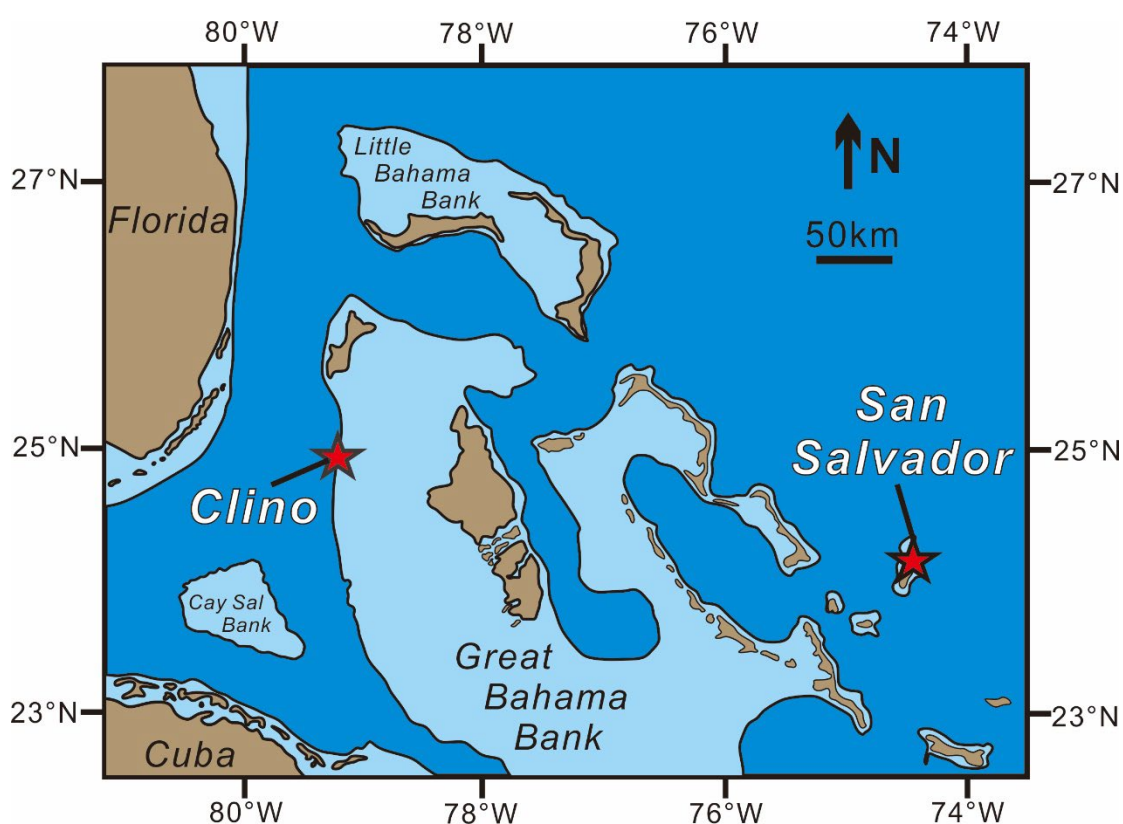


Fig. S1 Geological map and locations of drilling cores in the Bahamas.

2. Methods

2.1 X-ray diffraction

Small portions of each powdered sample were subject to X-ray diffraction (XRD) analysis utilizing a Panalytical X-pert Pro. In order to measure the abundance of dolomite and calcite, the samples were scanned between 23° and 72° in two-theta (2θ), using a step interval of 0.01° and a count time of 1 s for each step. The dolomite content was calculated using the area of the

appropriate peaks of calcite and dolomite obtained from six standards as described by Swart et al. (2002). The Corundum (Al_2O_3), as an internal standard, were baked at 100 to 105°C for 2 – 4 hours to remove absorbed H_2O and then was added to each sample to correct the parameter of d -spacing and two-theta values. The stoichiometry and cell parameters of dolomite crystals were calculated using the following equation from Lumsden and Chimahusky (1980).

$$N_{\text{CaCO}_3} = Md + B$$

Where the N_{CaCO_3} is the mole content of CaCO_3 (%), d is the corrected d -spacing of the dolomite by two internal standards, M is 333.33, and B is -911.999. The degree of cation ordering was determined by the ratio of peak [015] and [110] following the method of Goldsmith and Graf (1958).

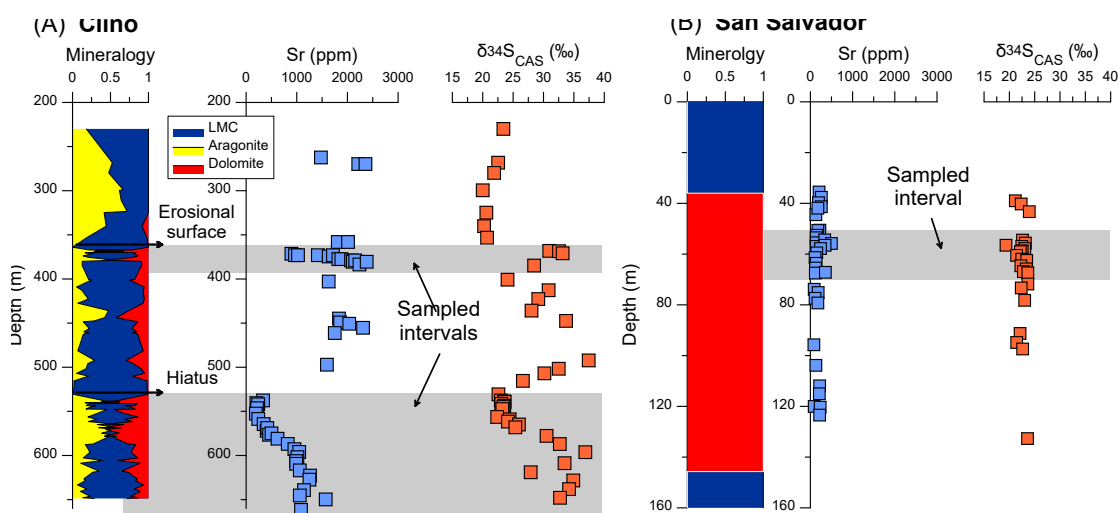


Fig. S2 The sampled intervals, mineralogy, Sr concentrations and $\delta^{34}\text{S}_{\text{CAS}}$ values in the Clino and San Salvador cores. The data of Sr concentrations and $\delta^{34}\text{S}_{\text{CAS}}$ values is from Murray et al. (2021)

2.2 Hydrogen peroxide treatment

In order to evaluate the influence of organic contamination associated, the hydrogen peroxide (3%) was treated to the Clino dolomite (Clino-1885.43-2AW) and the high-Mg calcite coral standard (echinophyllia) following the methods suggested by Zhang et al. (2019). In case of the possible isotopic exchange during the treatment experiment, each standard (50 mg) was soaked in the 10ml H_2O_2 solution for 12 and 24 hours respectively. The treated samples was dried in the oven at 40°C for 24 to 48 hours and then measured following the Section DR2.4. The results show that negligible differences within errors can be observed in the Δ_{47} and Δ_{48} values between treated and untreated samples and thus indicate the minor effect of organic materials on Δ_{47} and Δ_{48} values (Fig. S3 and

Table S1).

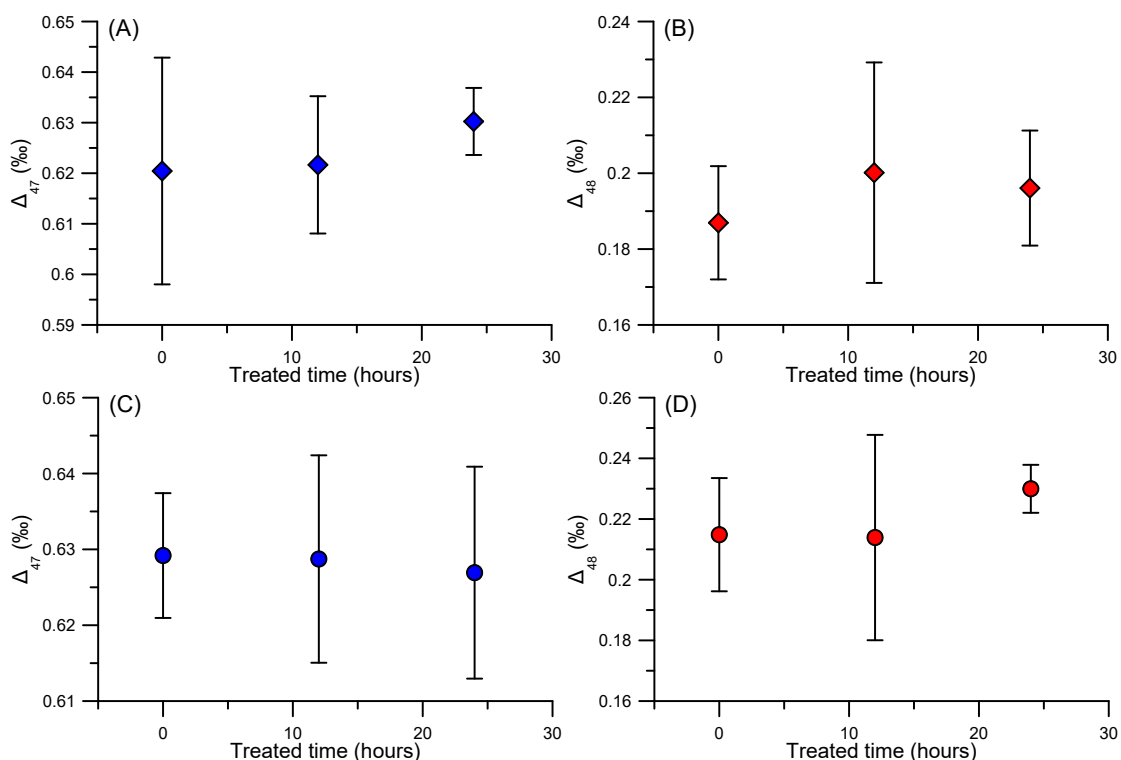


Fig. S3 The comparison of Δ_{47} and Δ_{48} values between treated and untreated standards. (A) and (B) The Δ_{47} and Δ_{48} values of the Clino dolomite treated by 12 and 24 hours compare with the untreated value. (C) and (D) The Δ_{47} and Δ_{48} values of the Bahamian coral sample treated by 12 and 24 hours compare with the untreated value.

2.3 Buffered acetic acid leaching method

The Clino samples are partially dolomitized and contained up to 50% calcite and in some instances also aragonite (Fig. S2A). In order to isolate dolomite, a buffered acetic acid leach was performed using the method outlined by Swart and Melim (2000). This method has been shown to reproduce the $\delta^{13}\text{C}_{\text{carb}}$, $\delta^{18}\text{O}_{\text{carb}}$ and Δ_{47} values of endmembers of soluble and insoluble carbonate minerals in modern and ancient carbonates (Lu et al., 2023; Murray et al., 2021). In this study, we also extended this method to the measurement of Δ_{48} values. During leaching processes, the less stable minerals, such as calcite and aragonite, are selectively dissolved leaving the dolomite in the residual material. After each leaching episode, the residual sample was rinsed twice using deionized water and dried in an oven for at least 24 hours at 40°C. After XRD diffraction (Section

DR2.1) and isotopic analyses of the dried residual sample (Section DR2.3), the procedure was repeated to obtain a more concentrated dolomite sample which was then reanalyzed. This step also can effectively clean the sample to remove the potential contamination, such as organic matters. While the final leached sample generally possesses between 90 - 100% dolomite, it is important not to completely remove all soluble materials (e.g., calcite and aragonite) in the first leaching step as this allows an intercept to be calculated which resultantly allow the stable isotopic values (Δ_{48} , Δ_{47} , $\delta^{13}\text{C}_{\text{carb}}$, and $\delta^{18}\text{O}_{\text{carb}}$ values) of the pure dolomite endmember to be estimated (Fig, S3). In order to test the effectiveness of this method for the dual clumped isotope measurements, a laboratory calcite standard (Carrara marble) was mixed with the dolomite standard (NIST-88b) to create a mixture of 61% dolomite and 39% calcite. This mixed sample was performed the acetic acid leaching procedure for five times to obtain a series of mixed samples with different contents of dolomite and calcite (Table S1). These resultant materials are ideal for the sensitive tests as they have different original $\delta^{18}\text{O}_{\text{carb}}$, Δ_{47} and Δ_{48} values.

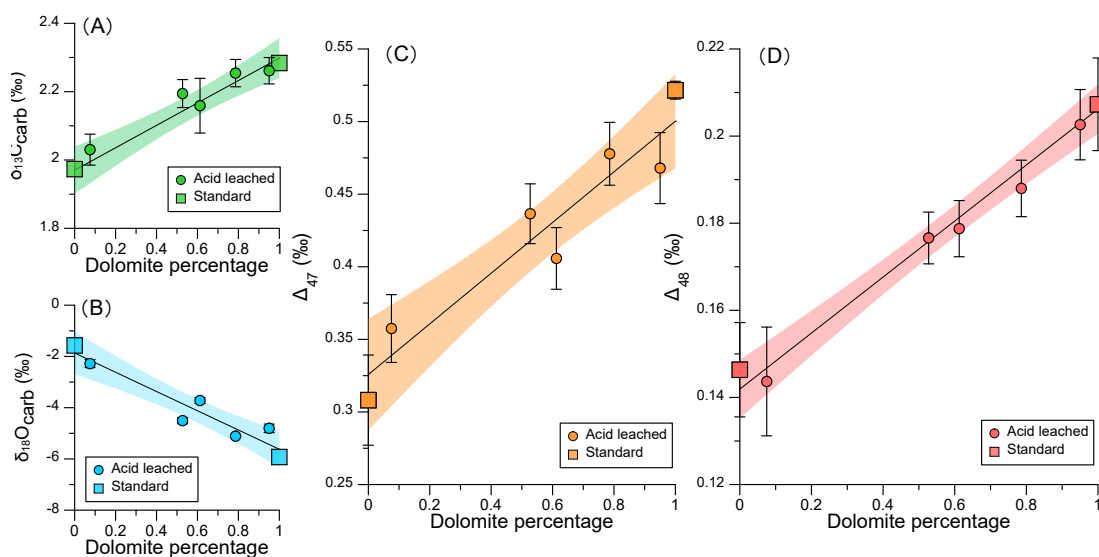


Fig. S4 The dependence of $\delta^{13}\text{C}_{\text{carb}}$, $\delta^{18}\text{O}_{\text{carb}}$, Δ_{47} and Δ_{48} values on dolomite percentages in the leached samples and standards of calcite (Carrara) and dolomite (NIST-88b). (A) $\delta^{13}\text{C}_{\text{carb}}$ values, (B) $\delta^{18}\text{O}_{\text{carb}}$ values, (C) Δ_{47} values, and (D) Δ_{48} values. The rectangle and cycle symbols respectively represent the standards and leached samples. The error bar of each sample is standard deviation. The shadow is 95% confidence.

The results of buffered acetic acid leaching experiments are presented in Fig. S4 and Tables S1, S6 and S7. The dependences of $\delta^{13}\text{C}_{\text{carb}}$, $\delta^{18}\text{O}_{\text{carb}}$, and Δ_{47} values on the dolomite percentage are well reproduced and are consistent with the results of Murray et al. (2021) (Fig. S3A, B and C). The

Δ_{48} values of the leached samples perfectly correlate with the dolomite contents (Fig. S4D). The endmember values extrapolated from the leached samples are consistent with the measured pure standards within 95% confidence (Fig. S4D).

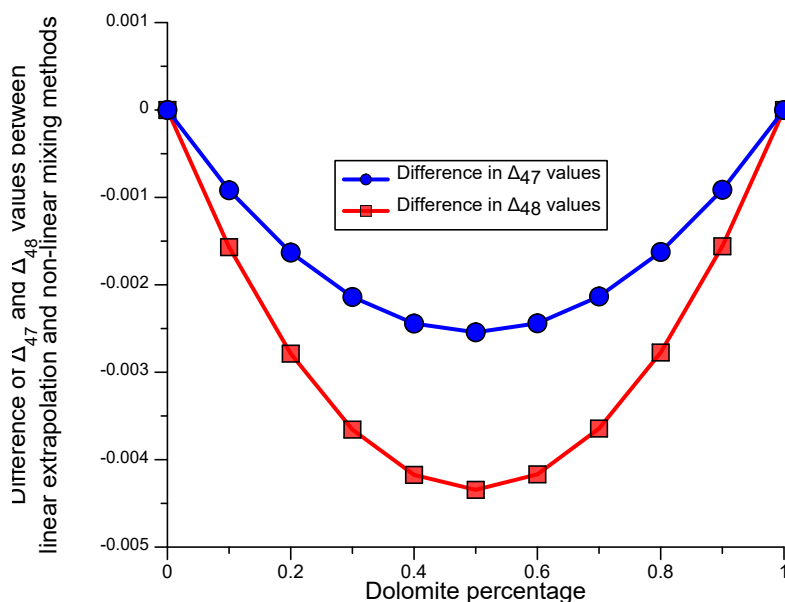


Fig. S5 The comparison of Δ_{47} and Δ_{48} values of the co-existing carbonates calculated by the linear extrapolation and non-linear mixing methods.

As the dolomite and the co-existing carbonates (aragonite and low-Mg calcites) in the Clino bulk samples have distinctive $\delta^{13}\text{C}_{\text{carb}}$, $\delta^{18}\text{O}_{\text{carb}}$, Δ_{47} and Δ_{48} values, this may induce the nonlinear mixing effect (Defliese and Lohmann, 2015; White and Defliese, 2023), which could produce the artificial Δ_{47} and Δ_{48} values of those two endmembers using the linear extrapolation of the leached samples. In this case, both the linear extrapolation and non-linear mixing methods are applicable. Because the differences in both Δ_{47} and Δ_{48} values of the co-existing carbonates are no more than 0.0025‰ for Δ_{47} values and 0.0042‰ for Δ_{48} values between those two methods (Fig. S4). Those differences produced by the different calculation methods are much smaller than the standard deviations of measurements for Δ_{47} (0.017‰) and Δ_{48} values (0.017‰).

2.4 Measurement evaluations

The methodology of stable and dual clumped isotopic measurements were established and systematically described by Swart et al. (2021). All the measurements of equilibrated, heated gases, standards and samples are presented in the Supplementary materials (Tables S3, S4, S5, S6, S7, S8,

S9 and S10).

2.4.1 Equilibrated and heated gases

In order to obtain the sufficient wide scale of δ^{48} values relative to the reference gas, two CO₂ standard gases (Tank A and Tank D) were equilibrated with the laboratory water standards (LS3, LS9, LS10, IAEA OH25 and IAEA OH27) with a wide range of $\delta^{18}\text{O}$ values (Table S2). From July 2021 to May 2022, we used the IAEA OH27 standard to equilibrate with gas standards. After May 2022, IAEA OH25 was to equilibrate with gas standards. For 25°C and 50°C equilibrated gases, we generally used the Tank A to equilibrate with the IAEA OH25 or OH27 and the Tank D to equilibrate with the LS3 and LS10. Generally, five to six gases were made for 1000°C equilibrium, including the Tank D equilibrated with the LS3, LS9 and LS10, the Tank A equilibrated with IAEA OH25 or OH27, and dried Tank A and D without any water equilibration. Those heated and equilibrated gases were monthly run for the CDES correction (Table S10).

All equilibrated gases were prepared in the stainless-steel extraction lines in the Stable Isotope Laboratory of the University of Miami. Aliquots of CO₂ standards were transferred into the Pyrex™ for 25°C and 50°C equilibrium and prebaked quartz tubes for 1000°C equilibrium. The Pyrex tubes were sealed using a gas torch and placed in the water bath for 25°C and 50°C equilibrium and the quartz tubes in muffle furnace for 1000°C equilibrium. The duration for the gas equilibrium was 3-4 hours for 1000°C, 1-3 days for 50°C, and 3-7 days for 25°C. After equilibration, the tube of 1000°C equilibrium was quenched (<30 seconds) at room temperature. For the 25°C and 50°C equilibrium gas standards, the tube was immediately moved into the methanol slush at -80°C to minimize any exchange of temperatures other than at the equilibration temperatures. The equilibrated gases then were attached into the extraction line and transferred the CO₂ gas for purification following the same protocol used for carbonate samples.

2.4.2 Purification and measurement

Between 8 - 10 mg of the powdered sample (< 0.074 mm) was digested in 3.5 cm³ of ~105% phosphoric acid (90°C) in a common acid bath for 20 - 30 minutes. The liberated CO₂ gas was continually trapped by liquid nitrogen through a methanol slush trap (-90°C) to remove the water for the first time. After the reaction was complete, a methanol slush bath (-90°C) was used to release the CO₂, which was cryogenically transferred to the second U-trap within the liquid nitrogen and freeze the residual water. The evolved CO₂ gas was then transferred through the third U-trap

filled with Porapak™ held between -25 and -30°C, a process that takes ~60 mins. The purified CO₂ was then frozen into a removable glass collection vessel which was, in turn, attached to the inlet of a Thermo Fisher MAT 253plus. During the whole extraction, two additional liquid nitrogen traps were used between the vacuum line and the turbomolecular pumps to avoid any back-streaming of contaminant species into extraction line. Between two purifications, the extraction line and the Poropak™ trap were respectively heated to 75°C and 150°C for 10 - 15 mins and cooled down at least 30 mins to the room temperature.

The analytical session of the MAT 253plus consists of 15 blocks of measurements between the analysis of the sample gas and an in-house reference “working gas”. The background was measured before (4.5 cycles) and after (4 cycles) each block following the framework of He et al. (2012). Measurements were performed at a voltage of 20,000 mV on the major ion beam with bellows compressed more than 35% compressed on both the sample and reference sides. This not only ensures the same amount of gas on both sides, but also a sufficient quantity that avoids artifacts during the measurement (Fiebig et al., 2019; Swart et al., 2021). The integration time is 14 seconds with 15 seconds delay time prior to each measurement. The total integration time for one sample measurements was 3150 seconds. This corresponding shot noise was calculated using the approach of Merritt and Hayes (1994) and is 0.006‰ for Δ_{47} and 0.019‰ for Δ_{48} .

2.4.3 Data corrections

2.4.3.1 $\delta^{13}\text{C}$ and $\delta^{18}\text{O}$ values

The $\delta^{13}\text{C}_{\text{carb}}$ and $\delta^{18}\text{O}_{\text{carb}}$ values of the reference gas were determined through the analysis of NBS-19 (National Bureau of Standards). To account for the differential fractionation between dolomite and calcite during the phosphoric acid digestion, a constant factor (-0.8‰) is used to correct the difference of $\delta^{18}\text{O}_{\text{carb}}$ values of dolomite relative to calcite (Sharma and Clayton, 1965).

2.4.3.2 Mass 47

For mass 47, a pressure baseline (PBL) correction applied to correct the negative baseline was only used to the correction of Δ_{47} values (He et al., 2012). Data reduction and normalization for the calculation of the raw Δ_{47} value followed the methodology of Huntington et al. (2009) and Daëron et al. (2016). Final Δ_{47} values were calibrated using both the Carbon Dioxide Equilibrium Scale (CDES) of Dennis et al. (2011) and the InterCarb CDES (I-CDES) of Bernasconi et al. (2021). The CDES was established using the heated and equilibrated gases. Changes in slopes and intercepts of δ^{47} and

Δ_{47} values from the 3 to 6 equilibrated gases were linearly interpolated to correct for the drift of measured samples during this period. For the I-CDES framework, the carbonate reference materials (ETH standards) were used to correct the Δ_{47} values of the experimental samples following the InterCarb method in Bernasconi et al. (2021). One of the ETH standards was processed daily with the full set of ETH standards (ETH-1, 2, 3 and 4) run each week. The ETH values averaged over a 30-day window. This generally included 8 to 12 measurements for ETH-1 together with ETH-2 standards and is consistent with the number of measurements ($n = 11$) made by Meckler et al. (2014). The linearity correction used ETH-1 and -2 combined with the “true values” from Bernasconi et al. (2021). The transfer function was based on the measurements of four carbonate standards (ETH-1, 2, 3 and 4). The reacting samples were regarded as the unknown values in a comparison of the CDES and I-CDES frameworks. During the analytical period, approximately 40% of all materials processed were either equilibrated gases or carbonate standards. All data corrected by the CDES and I-CDES frameworks are in Table S6, S7, S8 and S9. The difference in the Δ_{47} values calculated using the CDES and I-CDES corrections is $< 0.01\text{‰}$. The dependence of residuals of each ETH standard measurement relative to the theoretical value on the relative time is presented (Fig. S5 and S6, Table S8 and S9). The relative time is defined to the first time that we started to measure those dolomite samples. No significant drift can be recognized in the Δ_{47} values corrected by CDES and I-CDES frameworks (Fig. S5 and S6). Therefore, we used the Δ_{47} values corrected by the CDES method to be consistent with the Δ_{48} values. The temperatures were calculated from the Δ_{47} values using the equation established by Swart et al. (2019) at 90°C without acid fractionation factors (Lu et al., 2022).

2.4.3.3 Mass 48

For mass 48, the background was measured using the 47.5 half cup (Fiebig et al., 2019; Swart et al., 2021) and the PBL applied to the mass 48 peak. The data were then corrected to the CDES framework (Dennis et al., 2011) modified for mass 48 (Swart et al., 2021). While it is also possible to use a modified I-CDES approach for mass, this has not been used in this paper as there are still uncertainties regarding the precise Δ_{48} values for the ETH standards. No significant drift can be observed (Fig. S7). The averaged values of ETH standards are comparable to the values of Swart et al. (2021) and Fiebig et al. (2021) (Fig. S8).

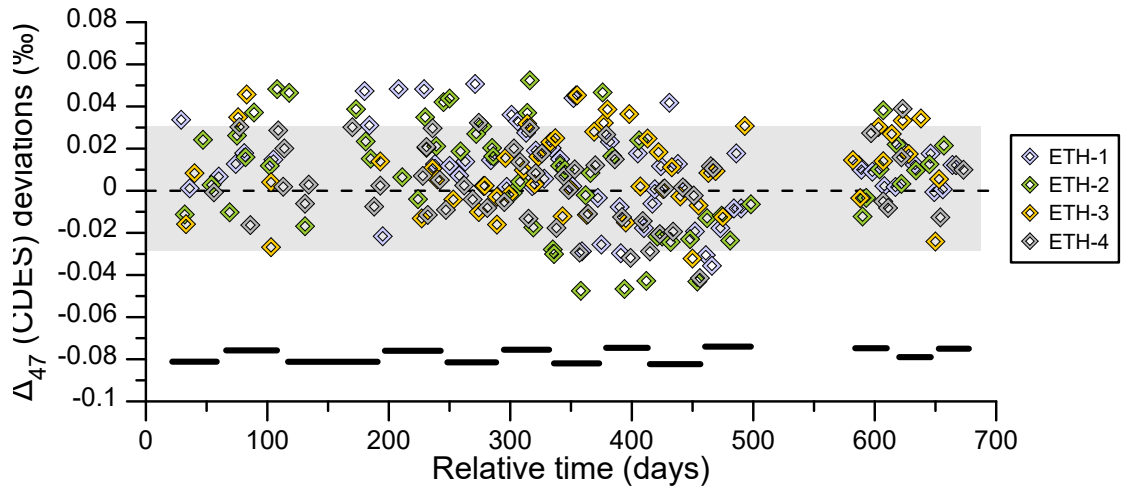


Fig. S6 The deviation of Δ_{47} values (CDES) relative to the theoretical value correlates to the relative time. The shadow represents the standard deviation (1se).

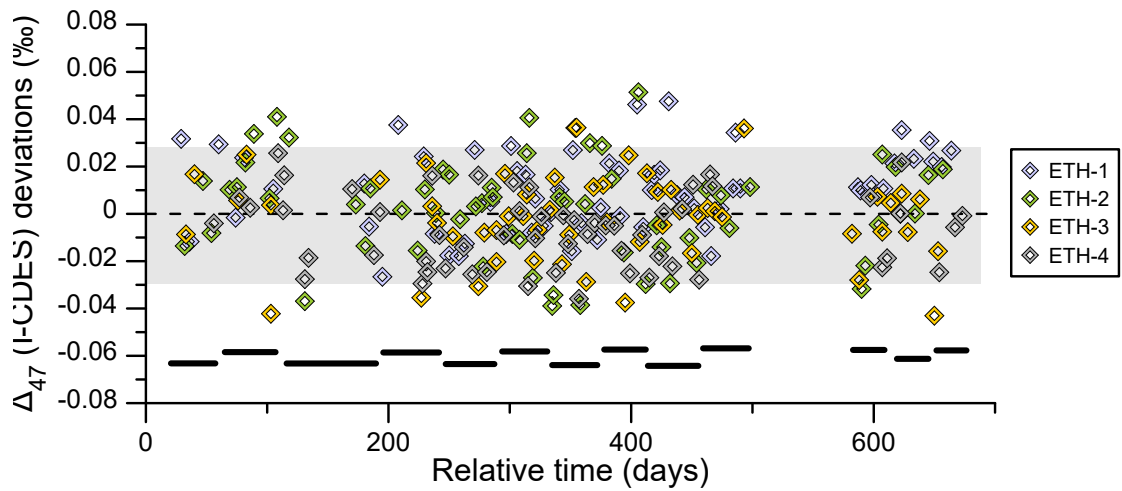


Fig. S7 The deviation of Δ_{47} values (I-CDES) relative to the theoretical value correlates to the relative time. The shadow represents the standard deviation (1se).

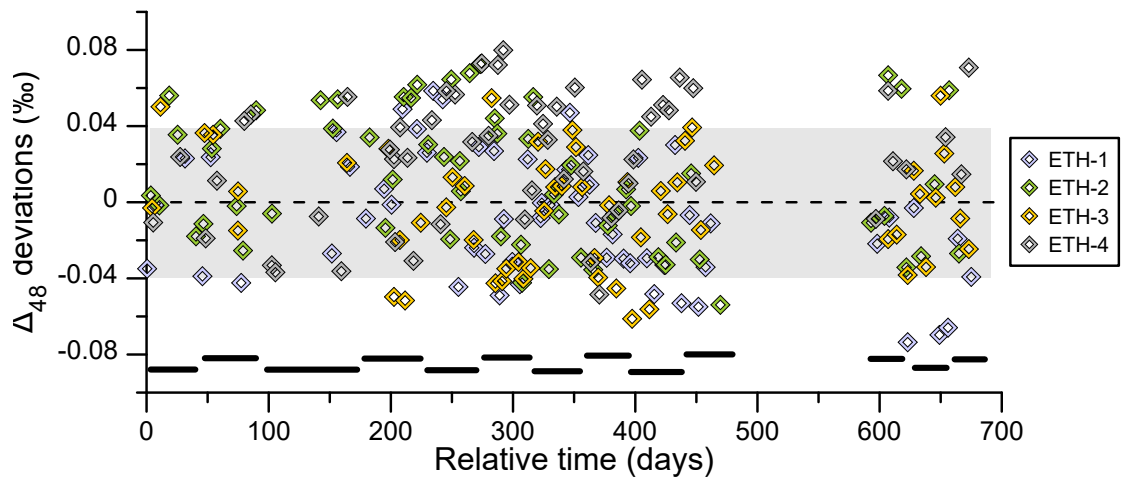


Fig. S8 The deviation of Δ_{48} values (CDES) relative to the theoretical value correlates to the relative time. The shadow represents the standard deviation (sd).

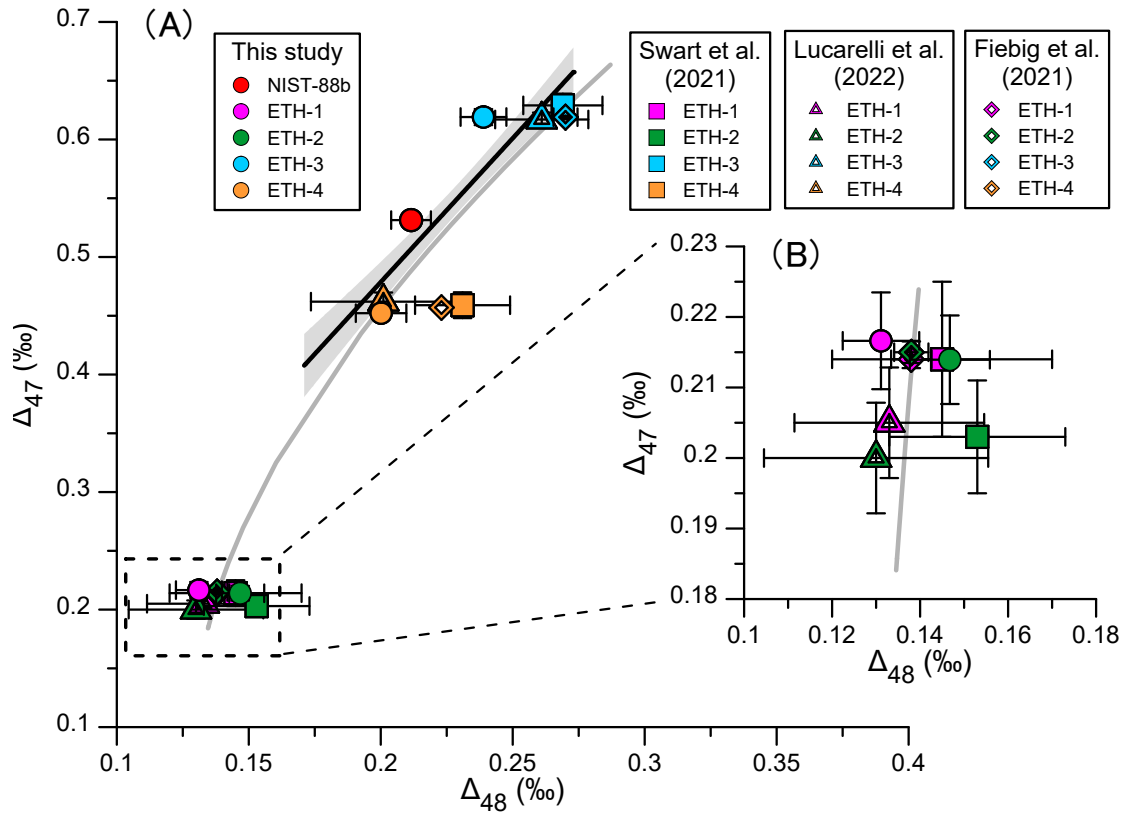


Fig. S9 Comparison of dolomite and calcite standards in the Δ_{47} - Δ_{48} framework. (A) The Δ_{47} and Δ_{48} values comparing with published data (Fiebig et al., 2021; Lucarelli et al., 2022; Swart et al., 2021). The red solid spot represents the dolomite standard (NIST-88b). (B) Zoom in to the Δ_{47} and Δ_{48} values of ETH-1 and ETH 2. The black line represents the Δ_{47} - Δ_{48} relationship derived from synthetic calcites (Swart et al., 2021). The grey line represents the theoretical relationship of Δ_{47} and Δ_{48} values (Hill et al., 2014)

2.5 IsoDIC model

This model has been developed in order to investigate changes of isotopic compositions (e.g., $\delta^{13}\text{C}$, $\delta^{18}\text{O}$, Δ_{47} , Δ_{48} and Δ_{49} values) of DIC during the processes including DIC- H_2O exchange, CO_2 degassing and absorption (Guo, 2020). The numerical framework has been applied to the interpretation of dual clumped isotopes in different carbonates, such as coral aragonites and cave calcites (Bajnai et al., 2020; Davies et al., 2022). Although the IsoDIC model has never been applied to the investigation of dolomite, the common sense is that the formation of dolomite responds to changes in carbonate (CO_3^{2-}) and/or bicarbonate concentrations (HCO_3^-) via CO_2 hydration in the dolomitizing fluid, which is a critical factor in the breakdown of the hydration of Mg ions with water (Gregg et al., 2015; Land, 1980; Machel and Mountjoy, 1986; Morrow, 1982; Vasconcelos et al., 1995).

In order to interpret the changes of Δ_{47} and Δ_{48} values in dolomite, three sets of boundary conditions were examined by the IsoDIC model as follows (Table 1):

1. The distinctive $\delta^{13}\text{C}$ values of DIC (0, -30 and -50‰) were assumed to examine the non-linear mixing effect on Δ_{47} and Δ_{48} values. The concentration of input carbonate ions is 2 mmol/kg in this model. The other parameters are defaulted (Table 1).

2. The effect of pH changes on the disequilibrium of Δ_{47} and Δ_{48} values during the CO_2 absorption is assessed. As previous studies suggested a wide range of pH during the formation of microbial dolomite, three groups of pH ranges are assumed and respectively correspond to the elevated (Group 1: 8.2 to 9) and depleted (Group 2: 6.5 to 7) ranges of pH as well as the normal seawater/marine porewater (Group 3: 7.8 to 8.2) (Table 1). The rest of parameters are constant in Table 1.

3. Two suits of carbonate ion (CO_3^{2-}) concentrations (Group 1: 2 to 5 mM and Group 2: 10 to 20 mM) were respectively performed in this model to evaluate the effect of DIC concentrations on the disequilibrium of Δ_{47} and Δ_{48} values during the CO_2 absorption. The pH is a constant value of 8.2. The temperature was mediated to 15°C as the mean temperature of porewater in the Bahamas (Eberli et al., 1997; Nagihara and Wang, 2000). The other parameters are default in this model (Table 1).

3. Stoichiometry, cation ordering, $\delta^{13}\text{C}_{\text{carb}}$, and $\delta^{18}\text{O}_{\text{carb}}$ values

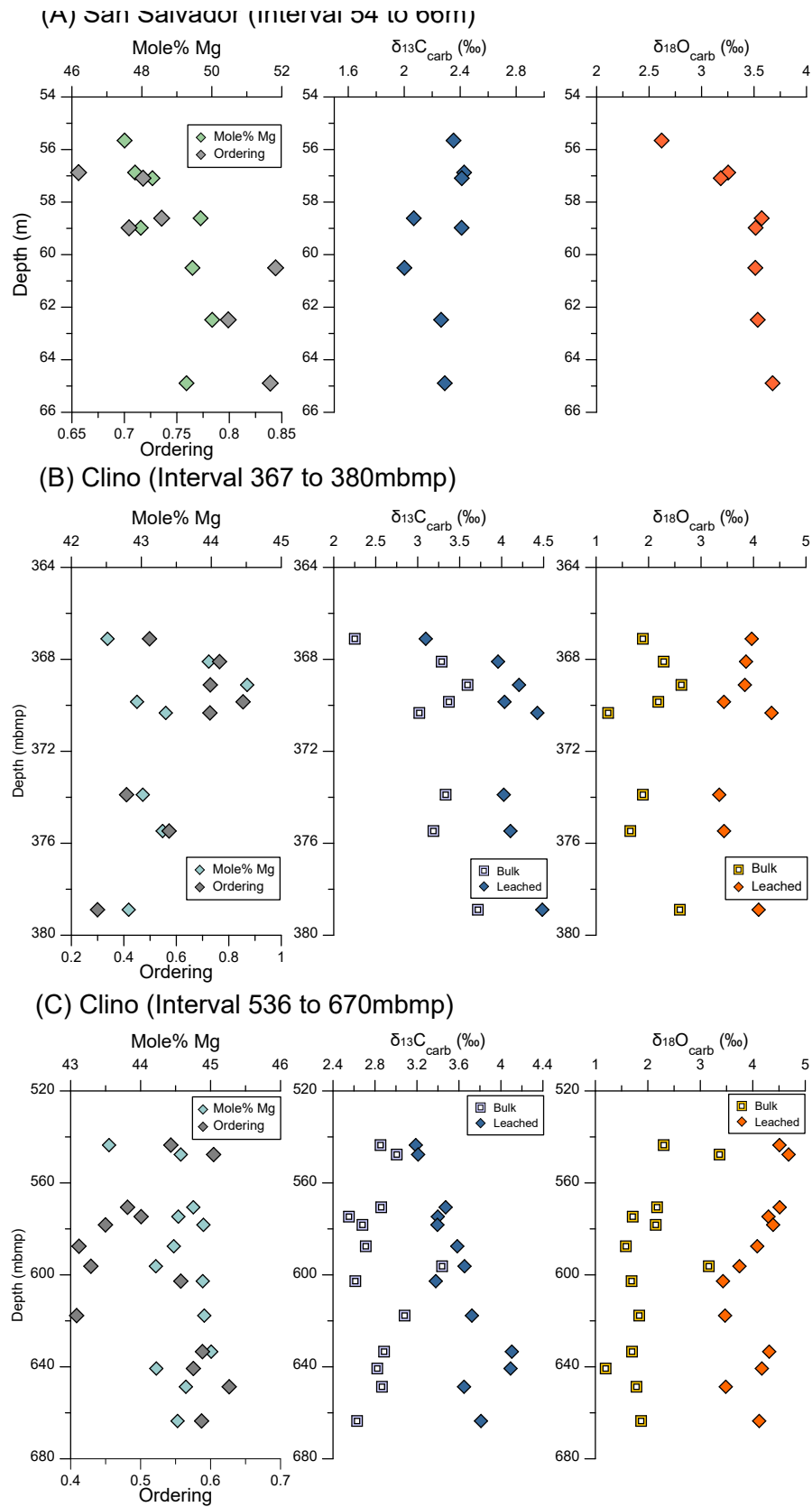


Fig. S10 The mol % Mg, cation ordering, $\delta^{13}\text{C}_{\text{carb}}$, $\delta^{18}\text{O}_{\text{carb}}$, Δ_{47} -temperature, and Δ_{48} -temperature

relative to depth. (A) Interval between 54 and 66 m in San Salvador. (B) and (C) Intervals 367 to 380 mbmp and 536 to 670 mbmp in Clino.

4. Effects of Mg^{2+} on Δ_{47} and Δ_{48} values

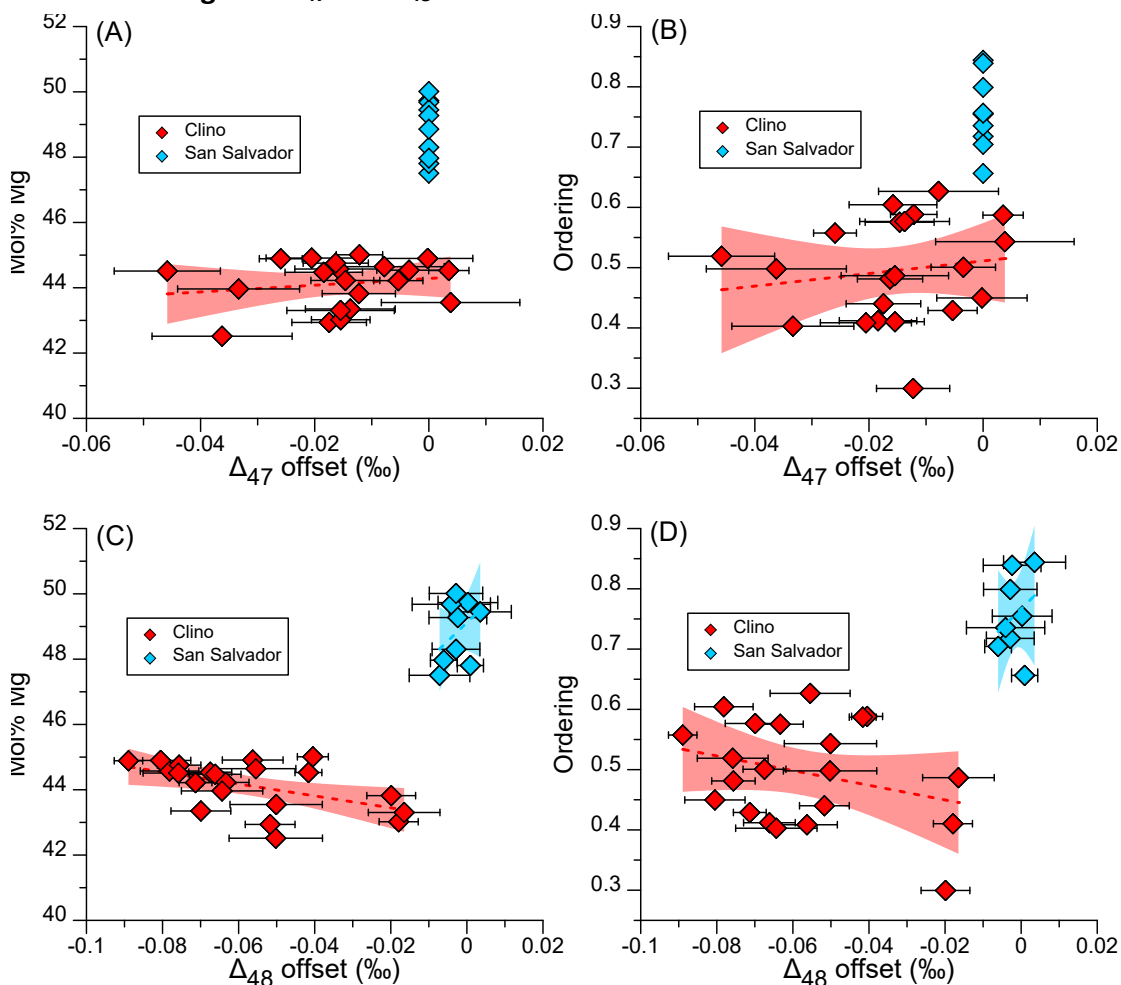


Fig. S11 The correlations of stoichiometry and cation ordering with the offsets of Δ_{47} and Δ_{48} between measured and expected values. The red and blue shadows represent the 95% confidence. The error bar represents standard error. (A) The cross plot between mol% Mg and the Δ_{47} offset in the Clino and San Salvador dolomites (R^2 of the Clino data is 0.03). (B) The crossplot between cation ordering and Δ_{47} offsets in the Clino and San Salvador dolomites (R^2 of the Clino samples is 0.02). (C) Crossplot between Mol% Mg and Δ_{48} offsets in the Clino and San Salvador dolomites. The R^2 of the Clino dolomite is 0.26. (D) Crossplot between cation ordering and Δ_{48} offsets in the Clino and San Salvador dolomites. The R^2 of the Clino dolomite is 0.08.

5. The $\delta^{34}S_{CAS}$ values and dolomite contents

The samples near the 568 and 368 mbmp hiatus show elevated $\delta^{34}S_{CAS}$ values which is correlated to the dolomite content (Fig. S10). This co-variation suggests the imprint of microbial sulfate reduction preserved in dolomite fraction of the bulk. In contrast, samples collected further away from the hiatus 368 mbmp or above the hiatus at 568 mbmp show relatively constant $\delta^{34}S_{CAS}$

values (Fig. S11).

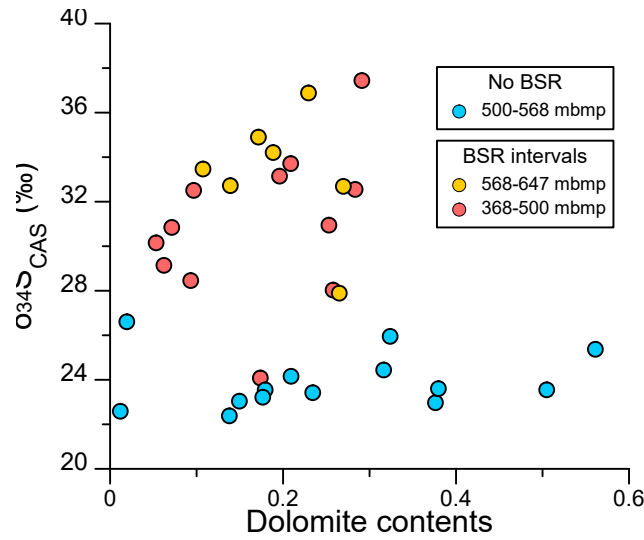


Fig. S12 Crossplot between $\delta^{34}\text{S}_{\text{CAS}}$ values and dolomite contents

6. Non-linear mixing effect of depleted $\delta^{13}\text{C}_{\text{carb}}$ values

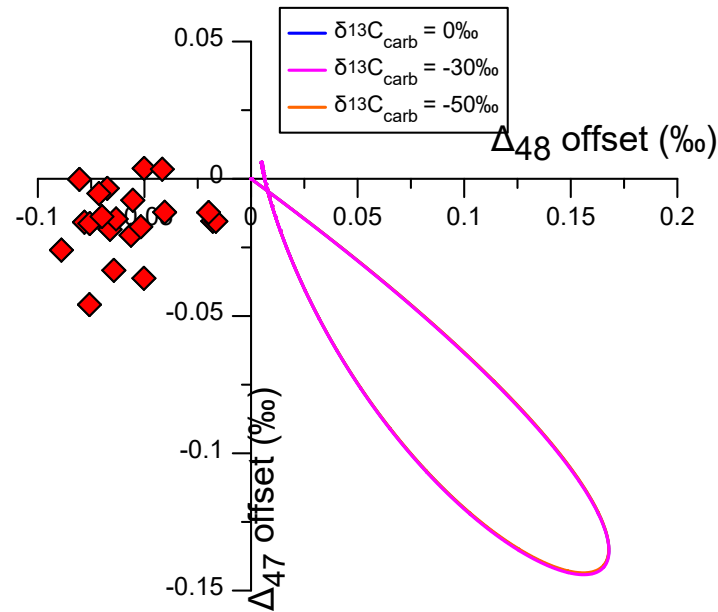


Fig. S13 The comparison of disequilibrium amplitude of Δ_{47} and Δ_{48} values between measured and modeled data shows the negligible difference in different $\delta^{13}\text{C}_{\text{carb}}$ values. The $\delta^{13}\text{C}_{\text{carb}}$ value derived from organic matters is respectively assumed to 0, -30 and -50‰. The input CO_3^{2-} concentration into the DIC pool is 2 mM. The modelled patterns with the range of $\delta^{13}\text{C}_{\text{carb}}$ values are overlapped.

7. Effects of pH and DIC concentrations on Δ_{47} and Δ_{48} values

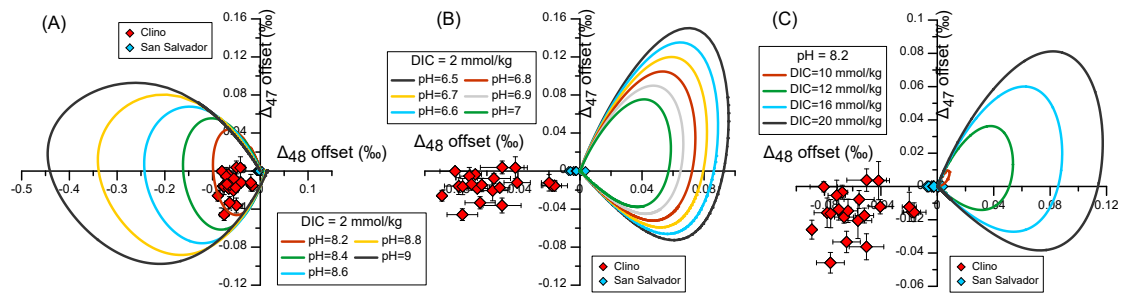


Fig. S14 The comparison between measured and modelled offsets of Δ_{47} and Δ_{48} values. (A) The modelled patterns in a high range of pH (8.2 to 9) compare with the measured Δ_{47} and Δ_{48} offsets. The DIC concentration is a constant (2mM) (B) The modelled patterns in a low range of pH (6.5 to 7) and a constant DIC concentration (2mM) compare with the measured the Δ_{47} and Δ_{48} offsets. (C) The modelled patterns in a high DIC concentrations (10 to 20 mM) compare with the measured Δ_{47} and Δ_{48} offsets. The pH is constant (8.2).

9. References

- Bajnai, D., Guo, W., Spotl, C., Coplen, T.B., Methner, K., Löffler, N., Krsnik, E., Gischler, E., Hansen, M., Henkel, D., Price, G.D., Raddatz, J., Scholz, D. and Fiebig, J. (2020) Dual clumped isotope thermometry resolves kinetic biases in carbonate formation temperatures. *Nature Communications* 11, 4005.
- Bernasconi, S.M., Daëron, M., Bergmann, K.D., Bonifacie, M., Meckler, A.N., Affek, H.P., Anderson, N., Bajnai, D., Barkan, E., Beverly, E., Blamart, D., Burgener, L., Calmels, D., Chaduteau, C., Clog, M., Davidheiser-Kroll, B., Davies, A., Dux, F., Eiler, J., Elliott, B., Fetrow, A.C., Fiebig, J., Goldberg, S., Hermoso, M., Huntington, K.W., Hyland, E., Ingalls, M., Jaggi, M., John, C.M., Jost, A.B., Katz, S., Kelson, J., Kluge, T., Kocken, I.J., Laskar, A., Leutert, T.J., Liang, D., Lucarelli, J., Mackey, T.J., Mangerot, X., Meinicke, N., Modestou, S.E., Müller, I.A., Murray, S., Neary, A., Packard, N., Passey, B.H., Pelletier, E., Petersen, S., Piasecki, A., Schauer, A., Snell, K.E., Swart, P.K., Tripathi, A., Upadhyay, D., Vennemann, T., Winkelstern, I., Yarian, D., Yoshida, N., Zhang, N. and Ziegler, M. (2021) InterCarb: A community effort to improve inter-laboratory standardization of the carbonate clumped isotope thermometer using carbonate standards. *Geochemistry, Geophysics, Geosystems* 22, e2020GC009588.
- Daëron, M., Blamart, D., Peral, M. and Affek, H.P. (2016) Absolute isotopic abundance ratios and the accuracy of Δ_{47} measurements. *Chemical Geology* 442, 83-96.
- Davies, A.J., Guo, W., Bernecker, M., Tagliavento, M., Raddatz, J., Gischler, E., Flögel, S. and Fiebig, J. (2022) Dual clumped isotope thermometry of coral carbonate. *Geochimica et Cosmochimica Acta* 338, 66-78.
- Dawans, J.M. and Swart, P.K. (1988) Textural and geochemical alternations in late Cenozoic Bahamian dolomites. *Sedimentology* 35, 385-403.
- Defliese, W.F. and Lohmann, K.C. (2015) Non-linear mixing effects on mass-47 CO_2 clumped isotope thermometry: Patterns and implications. *Rapid Communications in Mass Spectrometry* 29, 901-909.
- Dennis, K.J., Affek, H.P., Passey, B.H., Schrag, D.P. and Eiler, J.M. (2011) Defining an absolute reference frame for 'clumped' isotope studies of CO_2 . *Geochimica et Cosmochimica Acta* 75, 7117-7131.
- Eberli, G.P. (2000) 16. The Record of Neogene Sea-level Changes in the Prograding Carbonate along the Bahamas Transect—Leg 166 Synthesis1, *Proc ODP Sci Results, Leg. Eberli, G.P., Swart, P.K. and Malone, M.J. (1997) Proc. ODP, Init. Repts. 166.*
- Fiebig, J., Bajnai, D., Löffler, N., Methner, K., Krsnik, E., Mulch, A. and Hofmann, S. (2019) Combined high-precision Δ_{48} and Δ_{47} analysis of carbonates. *Chemical Geology* 522, 186-191.
- Fiebig, J., Daëron, M., Bernecker, M., Guo, W., Schneider, G., Boch, R., Bernasconi, S.M., Jautzy, J. and Dietzel, M. (2021) Calibration of the dual clumped isotope thermometer for carbonates. *Geochimica et Cosmochimica Acta* 312, 235-256.
- Gieskes, J.M., Elderfield, H. and Palmer, M.R. (1986) Strontium and its isotopic composition in interstitial waters of marine carbonate sediments. *Earth and Planetary Science Letters* 77, 229-235.
- Goldsmith, J.R. and Graf, D.L. (1958) Structural and Compositional Variations in Some Natural Dolomites. *The Journal of Geology* 66, 678-693.
- Gregg, J.M., Bish, D.L., Kaczmarek, S.E. and Machel, H.G. (2015) Mineralogy, nucleation and growth of dolomite in the laboratory and sedimentary environment: A review. *Sedimentology* 62, 1749-

1769.

Guo, W. (2020) Kinetic clumped isotope fractionation in the DIC-H₂O-CO₂ system: patterns, controls, and implications. *Geochimica et Cosmochimica Acta* 268, 230-257.

He, B., Olack, G.A. and Colman, A.S. (2012) Pressure baseline correction and high-precision CO₂ clumped-isotope (Δ_{47}) measurements in bellows and micro-volume modes. *Rapid Communications in Mass Spectrometry* 26, 2837-2853.

Huntington, K.W., Eiler, J.M., Affek, H.P., Guo, W., Bonifacie, M., Yeung, L.Y., Thiagarajan, N., Passey, B., Tripathi, A., Daeron, M. and Came, R. (2009) Methods and limitations of 'clumped' CO₂ isotope (Δ_{47}) analysis by gas-source isotope ratio mass spectrometry. *J Mass Spectrom* 44, 1318-1329.

Kenter, J.A.M., Ginsburg, R.N., Troelstra, S.R. and Ginsburg, R.N. (2001) Sea-Level-Driven Sedimentation Patterns on the Slope and Margin, Subsurface Geology of a Prograding Carbonate Platform Margin, Great Bahama Bank: Results of the Bahamas Drilling Project. *SEPM Society for Sedimentary Geology*, p. 61-100. Tulsa, USA.

Land, L.S. (1980) The isotopic and trace element geochemistry of dolomite: The state of the art. *SEPM Special Publications* 28, 87-110. Tulsa, USA.

Lu, C., Murray, S., Koeshidayatullah, A. and Swart, P.K. (2022) Clumped isotope acid fractionation factors for dolomite and calcite revisited: Should we care? *Chemical Geology* 588, 120637.

Lu, C., Zou, H., Wang, G., Cong, F., Quan, Y. and Swart, P.K. (2023) Clumped isotopes of paired dolomite and calcite constraining alteration histories of ancient carbonate successions. *Chemical Geology* 617, 121264.

Lucarelli, J.K., Carroll, H.M., Ulrich, R.N., Elliott, B.M., Coplen, T.B., Eagle, R.A. and Tripathi, A. (2022) Equilibrated gas and carbonate standard-derived dual (Δ_{47} and Δ_{48}) clumped isotope values. *Geochemistry, Geophysics, Geosystems*, 24, e2022GC010458.

Lumsden, D.N. and Chimahusky, J.S. (1980) Relationship between dolomite nonstoichiometry and carbonate facies parameters. *SEPM Special Publications*, 123-137. Tulsa, USA.

Machel, H.-G. and Mountjoy, E.W. (1986) Chemistry and Environments of Dolomitization —A Reappraisal. *Earth-Science Reviews* 23, p175-222.

McNeill, D.F., Eberli, G.P., Lidz, B.H., Swart, P.K., Kenter, J.A.M. and Ginsburg, R.N. (2001) Chronostratigraphy of a Prograded Carbonate Platform Margin: A Record of Dynamic Slope Sedimentation, Western Great Bahama Bank, Subsurface Geology of a Prograding Carbonate Platform Margin, Great Bahama Bank: Results of the Bahamas Drilling Project. *SEPM Society for Sedimentary Geology*, p. 101-121. Tulsa, USA.

McNeill, D.F., Ginsburg, R.N., Chang, S.-B.R. and Kirschvink, J.L. (1988) Magnetostratigraphic dating of shallow-water carbonates from San Salvador, Bahamas. *Geology* 16, 8-12.

Meckler, A.N., Ziegler, M., Millán, M.I., Breitenbach, S.F.M. and Bernasconi, S.M. (2014) Long-term performance of the Kiel carbonate device with a new correction scheme for clumped isotope measurements. *Rapid Communications in Mass Spectrometry* 28, 1705-1715.

Merritt, D.A. and Hayes, J.M. (1994) Factors Controlling Precision and Accuracy in Isotope-Ratio-Monitoring Mass Spectrometry. *Analytical Chemistry* 66, 2336-2347.

Morrow, D.W. (1982) Dolomitization models and ancient dolostones. *Geosci. Canada* 9, 107.

Murray, S.T., Higgins, J.A., Holmden, C., Lu, C. and Swart, P.K. (2021) Geochemical fingerprints of dolomitization in Bahamian carbonates: Evidence from sulphur, calcium, magnesium and clumped isotopes. *Sedimentology* 68, 1-29.

Murray, S.T. and Swart, P.K. (2017) Evaluating formation fluid models and calibrations using

clumped isotope paleothermometry on Bahamian dolomites. *Geochimica et Cosmochimica Acta* 206, 73-93.

Nagihara, S. and Wang, K. (2000) Geothermal Regime of the Western Margin of the Great Bahama Bank, Proceedings of the Ocean Drilling Program. Scientific results. Ocean Drilling Program, pp. 113-120.

Sharma, T. and Clayton, R.N. (1965) Measurement of $^{18}\text{O}^{16}\text{O}$ ratios of total oxygen of carbonates. *Geochimica et Cosmochimica Acta* 29, 1347-1353.

Swart, P.K., James, N.P., Mallinson, D., Malone, M.J., Matsuda, H. and Simo, T. (2002) 10. Data Report: Carbonate Mineralogy of Sites Drilled during Leg 182.

Swart, P.K., Lu, C., Moore, E.W., Smith, M.E., Murray, S.T. and Staudigel, P.T. (2021) A calibration equation between Δ_{48} values of carbonate and temperature. *Rapid Communications in Mass Spectrometry* 35, e9147.

Swart, P.K. and Melim, L.A. (2000) The Origin of Dolomites in Tertiary Sediments from the Margin of Great Bahama Bank. *Journal of Sedimentary Research* 70, 738-748.

Swart, P.K., Murray, S.T., Staudigel, P.T. and Hodell, D.A. (2019) Oxygen Isotopic Exchange between CO_2 and Phosphoric Acid: Implications for the Measurement of Clumped Isotopes in Carbonates. *Geochemistry, Geophysics, Geosystems* 20, 3730-3750.

Swart, P.K., Ruiz, J. and Holmes, C.W. (1987) Use of strontium isotopes to constrain the timing and mode of dolomitization of upper Cenozoic sediments in a core from San Salvador, Bahamas. *Geology* 15, 262-265.

Vahrenkamp, V.C., Swart, P.K. and Ruiz, J. (1991) Episodic dolomitization of late Cenozoic carbonates in the Bahamas; evidence from strontium isotopes. *Journal of Sedimentary Research* 61, 1002-1014.

Vasconcelos, C., McKenzie, J.A., Bernasconi, S., Grujic, D. and Tiens, A.J.J.N. (1995) Microbial mediation as a possible mechanism for natural dolomite formation at low temperatures. *Nature* 377, 220-222.

White, J.H. and Defliese, W.F. (2023) $\delta^{13}\text{C}$ and $\delta^{18}\text{O}$ heterogeneities in carbonates: Nonlinear mixing in the application of dual-carbonate-clumped isotope thermometer. *Rapid Communications in Mass Spectrometry* 37, e9627.

Zhang, N., Lin, M., Yamada, K., Kano, A., Liu, Q., Yoshida, N. and Matsumoto, R. (2019) The effect of H_2O_2 treatment on stable isotope analysis ($\delta^{13}\text{C}$, $\delta^{18}\text{O}$ and Δ_{47}) of various carbonate minerals. *Chemical Geology*, 119352.